

Implementation of a drive system for dual single-phase induction motor using a five-leg inverter with carrier-based space vector PWM technique

Abstract. This paper presents the implementation of a drive system of a dual single-phase induction motor system with independently closed loop speed control using a five-leg voltage source inverter. Simple closed-loop speed V/f scalar control method and carrier-based space vector PWM (SVPWM) are implemented on dSPACE DS1104. The details of dSPACE configuration and programming are fully given. The experimental results show that the implemented system is able to independently control to keep speed constant for each motor under various operating conditions.

Streszczenie. W pracy przedstawiono implementację układu napędowego podwójnego jednofazowego silnika indukcyjnego z niezależną kontrolą prędkości w zamkniętej pętli za pomocą pięciostopniowego falownika ze źródłem napięcia. Prosta metoda kontroli skalarnego prędkości V/f w pętli zamkniętej i oparty na nośnej wektor przestrzeni PWM (SVPWM) są zaimplementowane na dSPACE DS1104. Szczegóły konfiguracji i programowania dSPACE są w pełni podane. Wyniki eksperymentów pokazują, że wdrożony system jest w stanie niezależnie kontrolować, aby utrzymać stałą prędkość dla każdego silnika w różnych warunkach pracy. (Opracowanie systemu napędowego dla podwójnego jednofazowego silnika indukcyjnego z pięciostopniowym falownikiem z techniką PWM opartą na nośniku wektorowym)

Keywords: Five-leg voltage source inverter; Dual single-phase induction motor; Carrier-based space vector PWM;

Słowa kluczowe: Pięciostopniowy falownik źródła napięcia; Podwójny jednofazowy silnik indukcyjny; Wektor przestrzenny oparty na nośnej PWM;

Introduction

In recent years research of variable speed multi-motor drive systems using voltage source inverters (VSIs) with a common leg has been paid attention since high efficiency, high performance, and low cost ac motor drive system are required for many industrial applications [1, 10, 11, 12]. A five-leg inverter PWM technique for reduced switch two-motor constant power applications like centre-driven winders has been proposed [2, 15]. The five-leg VSI modified from two-three leg VSIs by using the same capacitor and dc bus offers reductions in the size, number of devices, losses of the inverters, and capital cost [1]. Also the numbers of microcontrollers and driver circuits are reduced. However these publications are concerned with two three-phase induction motors. There are a few publications of driving two single-phase induction motors using the five-leg VSI. A single-phase induction motor is normally used in home appliances for low power such as pumps, fans, air conditioners and so on. Variable speed drives with a three-leg VSI for an asymmetrical type two-phase induction motor modified from the single-phase induction motor for improved performance such as torque pulsations can be found in [3, 4, 5, 6, 7]. The three-leg VSI for two-phase motors is more required when compared to other topologies such as two-leg and four leg VSIs in terms dc bus utilization and ease of SVPWM implementation [3, 4, 6, 17]. A carrier based SVPWM technique for three-leg VSI fed asymmetrical type two-phase induction motor is well established [3]. However the carrier based SVPWM technique for five-leg VSI driven two single-phase induction motors has not been reported yet. Moreover, advanced speed control for a five-leg VSI driving a dual-induction motor system is somewhat complicated [1, 16]. It is suitable for high power applications. For low power applications, simple closed loop speed control for the two single-phase induction motors seems to be preferable because of low cost [9]. More importantly, the five-leg VSI fed dual single-phase induction motor can meet the objectives like a high power dual three-phase induction motor system. Therefore this paper will focus on describing the principle and implementation of carrier-based SVPWM for the five-leg VSI developed from patterns for two three-leg VSIs using

six-legs. Simple closed-loop speed V/f scalar control method is used for independent control of dual single-phase induction motor. Both control method and SVPWM are implemented on dSPACE DS1104.

Figure 1 demonstrates the proposed five-leg voltage source inverter for driving dual single-phase induction motor (M1 and M2). There is one inverter leg acting as a common leg. The motor specification is 370W, 230V, 50Hz, 2 pole-pairs and it has two stator windings so called auxiliary winding and main winding. When the independent reference speed commands are set for both motors, the V/f control is used for generating PWM patterns for five legs with a common leg instead of six legs of the inverter. Principle of generating SVPWM for five legs will be described in the next section.

Carrier based SVPWM

Conventional two three-leg VSIs with individual DC source inputs and controllers supplying two single-phase induction motors with independent control is shown in Fig.2. For a carrier based SVPWM technique, modulating or reference signals are required to be compared with a common triangular wave as a carrier. The reference signals for six legs of the two inverters for both motors can be expressed as follows:

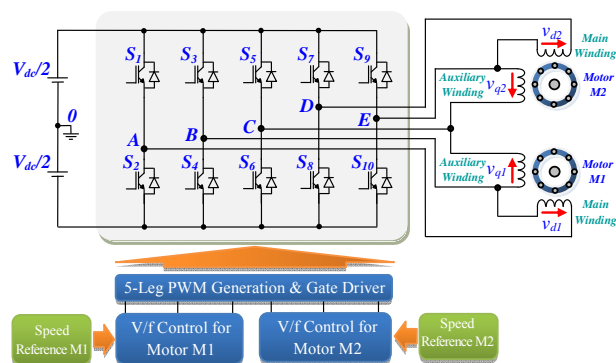


Fig. 1. Proposed system for driving dual single-phase motor.

- (1) $v_{a1,ref}^* = M_{a1} \sin(\omega_1 t) + v_{zero1}^* = v_{a1,ref} + v_{zero1}^*$
- (2) $v_{b1,ref}^* = M_{a1} \sin\left(\omega_1 t - \frac{\pi}{2}\right) + v_{zero1}^* = v_{b1,ref} + v_{zero1}^*$
- (3) $v_{c1,ref}^* = M_{a1} \sin(\omega_1 t - \pi) + v_{zero1}^* = v_{c1,ref} + v_{zero1}^*$
- (4) $v_{a2,ref}^* = M_{a2} \sin(\omega_2 t) + v_{zero2}^* = v_{a2,ref} + v_{zero2}^*$
- (5) $v_{b2,ref}^* = M_{a2} \sin\left(\omega_2 t - \frac{\pi}{2}\right) + v_{zero2}^* = v_{b2,ref} + v_{zero2}^*$
- (6) $v_{c2,ref}^* = M_{a2} \sin(\omega_2 t - \pi) + v_{zero2}^* = v_{c2,ref} + v_{zero2}^*$

where: $v_{a1,ref}, v_{b1,ref}, v_{c1,ref}$, are the fundamental reference voltages for a three-leg VSI fed single-phase induction motor M1, $v_{a2,ref}, v_{b2,ref}, v_{c2,ref}$ are the fundamental reference voltages for the another three-leg VSI fed single-phase induction motor M2, and v_{zero1}^* and v_{zero2}^* are the zero sequence reference voltages for M1 and M2, respectively. M_{a1} and M_{a2} are the modulation index for M1 and M2, respectively, ω_1 and ω_2 are the angular frequency for each motor.

The advantage of adding the zero sequence reference voltages v_{zero1}^* and v_{zero2}^* to (1) to (6) is that it can help to reduce lower harmonic currents and increase higher available modulation index, when compared to the sinusoidal PWM (SPWM) technique [17]. The zero sequence reference voltage can be expressed as:

- (7) $v_{zero1}^* = \left[\frac{\max(v_{a1,ref}, v_{b1,ref}, v_{c1,ref}) + \min(v_{a1,ref}, v_{b1,ref}, v_{c1,ref})}{2} \right]$
- (8) $v_{zero2}^* = \left[\frac{\max(v_{a2,ref}, v_{b2,ref}, v_{c2,ref}) + \min(v_{a2,ref}, v_{b2,ref}, v_{c2,ref})}{2} \right]$

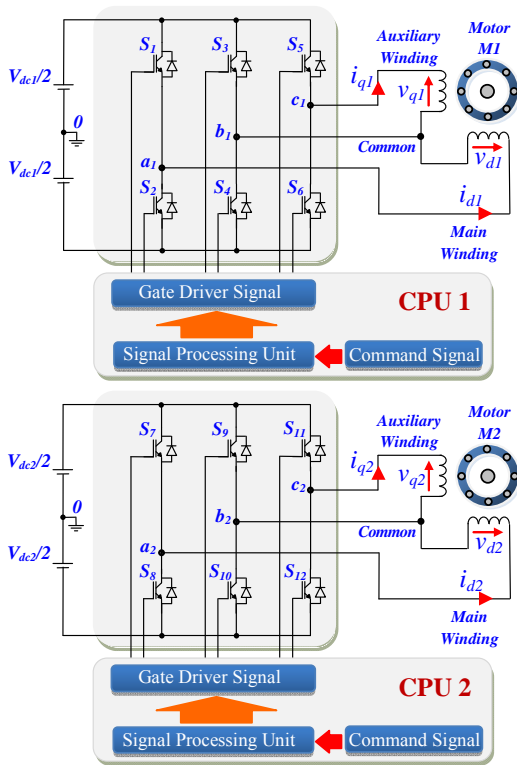


Fig. 2. Conventional two three-leg VSIs and their controllers for two single-phase induction motors with independent control.

The winding reference voltages for both motors can be expressed as follows:

- (9) $v_{d1,ref}^* = v_{a1,ref}^* - v_{b1,ref}^*$
- (10) $v_{q1,ref}^* = v_{c1,ref}^* - v_{b1,ref}^*$
- (11) $v_{d2,ref}^* = v_{a2,ref}^* - v_{b2,ref}^*$
- (12) $v_{q2,ref}^* = v_{c2,ref}^* - v_{b2,ref}^*$

where: $v_{d1,ref}^*, v_{q1,ref}^*$ are the balanced two-phase output reference voltages for the three-leg fed single-phase induction motor M1, $v_{d2,ref}^*, v_{q2,ref}^*$ are the balanced two-phase output reference voltages for the three-leg fed single-phase induction motor M2.

If two three-leg VSIs are used for driving especially two single-phase induction motors, required six phase leg reference voltages are $v_{a1,ref}^*, v_{b1,ref}^*, v_{c1,ref}^*$ for M1 and $v_{a2,ref}^*, v_{b2,ref}^*, v_{c2,ref}^*$ for M2. These reference voltages can be reduced from six modulating signals to five modulating signals for the five-leg VSI by using phase leg C as a common leg sharing currents for both motors as follows:

- (13) $v_{A,ref}^* = v_{A0} / v_{dc} = (v_{a1,ref}^* + v_{c2,ref}^*) / 2$
- (14) $v_{B,ref}^* = v_{B0} / v_{dc} = (v_{b1,ref}^* + v_{c2,ref}^*) / 2$
- (15) $v_{C,ref}^* = v_{C0} / v_{dc} = (v_{c1,ref}^* + v_{c2,ref}^*) / 2$
- (16) $v_{D,ref}^* = v_{D0} / v_{dc} = (v_{a2,ref}^* + v_{c1,ref}^*) / 2$
- (17) $v_{E,ref}^* = v_{E0} / v_{dc} = (v_{b2,ref}^* + v_{c1,ref}^*) / 2$

For the five-leg VSI, the winding reference voltages for both motors can be expressed as follows:

- (18) $v_{d1,ref}^* = v_{A,ref}^* - v_{B,ref}^* = \frac{1}{\sqrt{2}} M_{a1} \sin\left(\omega_1 t + \frac{\pi}{4}\right)$
- (19) $v_{q1,ref}^* = v_{C,ref}^* - v_{B,ref}^* = \frac{1}{\sqrt{2}} M_{a1} \sin\left(\omega_1 t + \frac{3\pi}{4}\right)$
- (20) $v_{d2,ref}^* = v_{D,ref}^* - v_{E,ref}^* = \frac{1}{\sqrt{2}} M_{a2} \sin\left(\omega_2 t + \frac{\pi}{4}\right)$
- (21) $v_{q2,ref}^* = v_{C,ref}^* - v_{E,ref}^* = \frac{1}{\sqrt{2}} M_{a2} \sin\left(\omega_2 t + \frac{3\pi}{4}\right)$

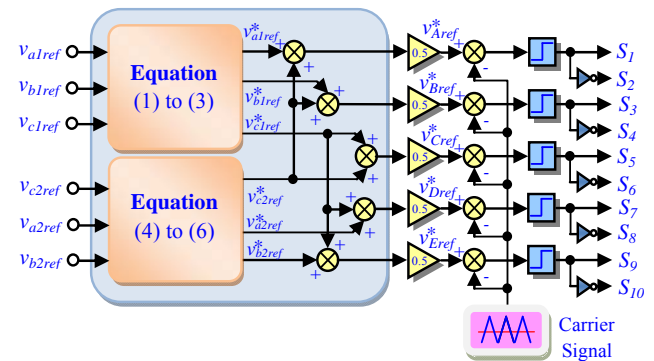


Fig. 3. Carrier-based SVPWM modulator for five-leg VSI.

The generation of the carrier-based SVPWM signals by using (13) to (17) to be compared with the carrier for a five-leg VSI can be obviously represented as shown in Fig. 3. $S_1, S_3, S_5, S_7,$ and S_9 are switching signals for upper switching devices whilst $S_2, S_4, S_6, S_8,$ and S_{10} are switching signals for lower switching devices of phase leg a, b, c, d, e, respectively.

Fig. 4 shows the pattern of the carrier-based SVPWM signals for controlling the five-leg VSI when the reference speed of M1 is set at 1500 rpm and the reference speed of M2 is set at 750 rpm. Fig. 4 (a) shows the pattern of five signals of reference voltages. When these reference voltages are compared to the carrier with frequency of f_c , the output PWM signals are generated to enable switches producing the phase leg voltages v_{A0} to v_{E0} as Fig. 4 (b) to (f). Fig. 4 (g) to (j) show the waveforms of winding voltages v_d and v_q for each motor by using (9) and (12). Clearly the fundamental frequency for M1 is twice that for M2 in accordance with the speed command for both motors.

Dspace configuration and programming

Block diagram of the closed-loop speed V/f control system is shown in Figure 5 for generating the terminal voltages for dual single-phase induction motor with independent two PI speed controllers. The whole system real time model can be implemented in a MATLAB/Simulink environment as shown in Figure 6. Software implementation is programmed on a dSPACE DS1104 DSP controller board with TMS320F240 slave DSP for producing carrier-based SVPWM signals for the five-leg VSI and closed loop speed control for both motors.

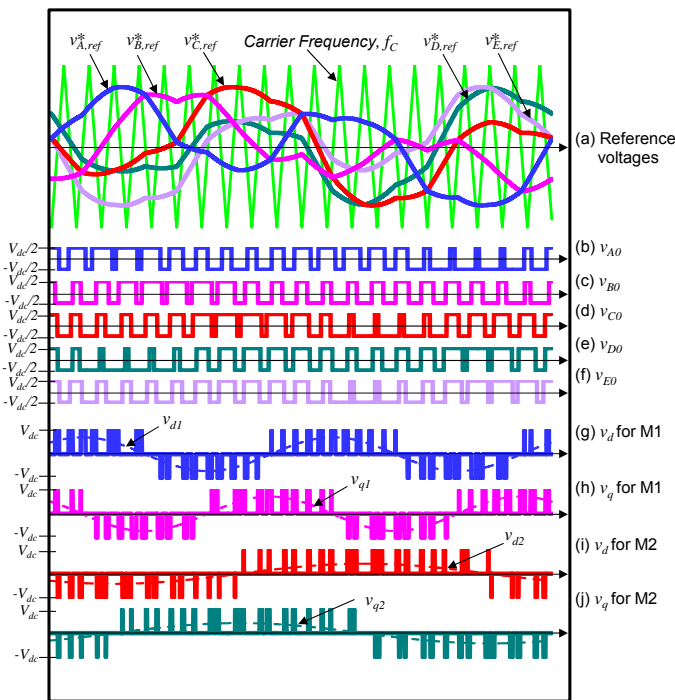


Fig. 4. Proposed SVPWM pattern for the five-leg VSI.

Figs. 7 and 8 show inside of the block "Actual speed M1 (or M2)". These blocks read actual speed values of M1 and M2 via ADC blocks, which are 12-bits ADC ports. Filter transfer function is used to reduce the noise from speed signals. DAC blocks which are 12-bits DAC ports, are used to display output actual speed signals at a digital oscilloscope.

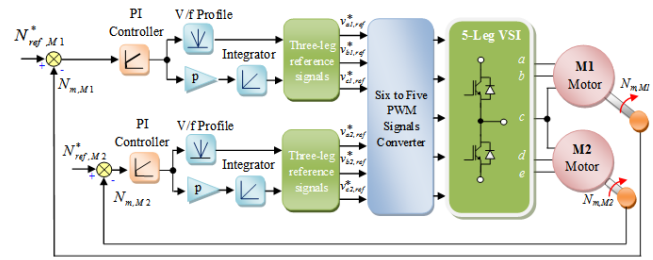


Fig. 5. Closed-loop speed v/f controller for five-leg VSI.

The speed error between the reference speed and the actual speed is obtained by using a summing block in Fig. 6. These speed errors are fed to calculate with discrete proportional and integral gains of speed controllers in the block "PI Speed Controller" as shown in Figs. 9 and 10.

The output of the PI controller is fed to the block "V/f for M1 (or M2)". The calculation inside these blocks is shown in Figs. 11 and 12. Adding a speed limit block can prevent anti-windup from the PI controller. The output of this block is used for defining the modulating index, M_u and angular displacement, θ_s for reference signals.

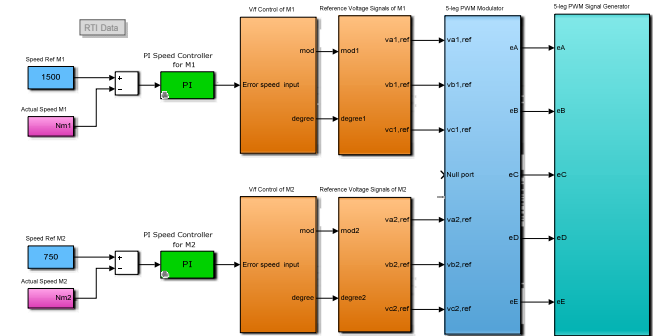


Fig. 6. Overall closed-loop speed control system block diagram using Matlab/Simulink for driving two sets of 1- phase induction motor.

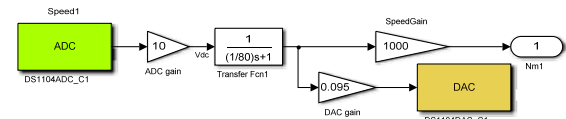


Fig. 7. Inside of the block "Actual speed M1".

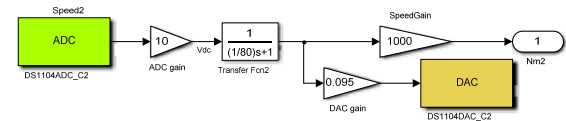


Fig. 8. Inside of the block "Actual speed M2".

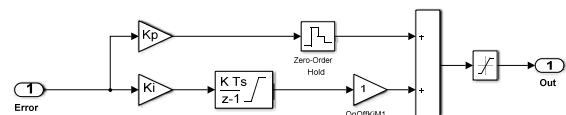


Fig. 9. Inside of the block "PI Speed Controller for M1".

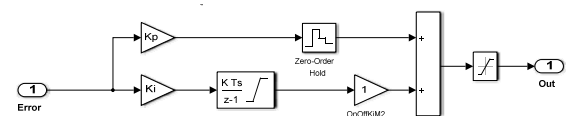


Fig. 10. Inside of the block "PI Speed Controller for M2".

Each V/F lookup table block for M1 and M2 is determined in accordance with the following equation:

$$(22) \quad M_a = \frac{V_s}{f_s}$$

The modulation index, M_a is related to the ratio of voltage and frequency and varied between 0 to 1 for a linear range. Due to the balanced voltages applied, the slope of the V/f profile in the table block "V/F table M1 (or M2)" for the main winding voltage and the auxiliary winding voltage are similar.

For calculating angular displacement, θ_s , the command speed, N_{ref}^* can be expressed as:

$$(23) \quad \theta_s = \int \frac{p \cdot N_{ref}^* \cdot 2\pi}{60} dt + C$$

where: C is a constant for an initial value of the integration, p is the number pole pairs.

By using (13) to (17), the six reference voltage signals are combined and reduced to five duty cycle signals, as shown inside the block "5-leg PWM Modulator" in Fig. 15.

After determining M_a and θ_s values, using (1) to (6) yields the reference voltages by adding zero reference voltages for each single-phase motor as shown inside the block "Reference Voltage signals of M1 (or M2) in Figs. 13 and 14.

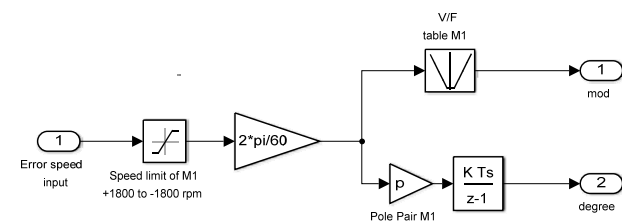


Fig. 11. Inside the block "V/f Control for M1".

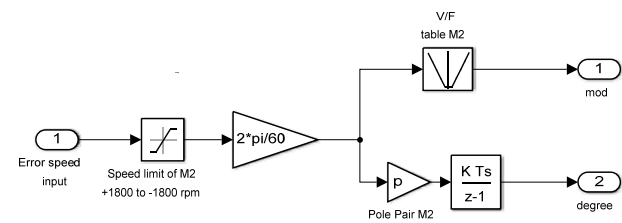


Fig. 12. Inside the block "V/f Control for M2".

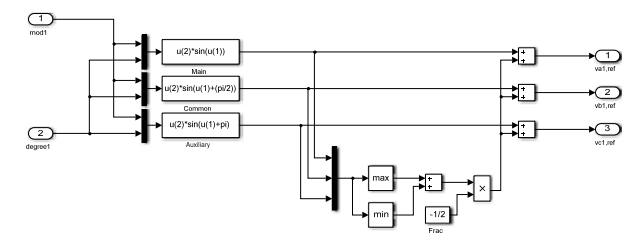


Fig. 13. Inside the block "Reference Voltage Signals of M1".

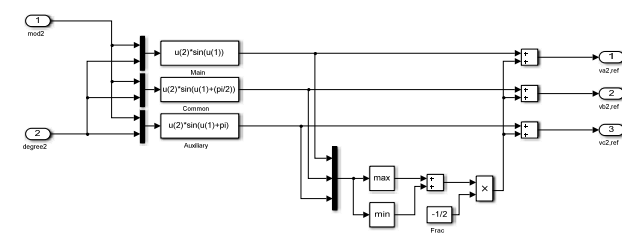


Fig. 14. Inside the block "Reference Voltage Signals of M2".

Thus, Fig. 16 shows the inside of the block "5-leg PWM signal generator". Inside this block, the five reference voltage signals (+1 p.u.) is reduced to a half (+0.5 p.u.) and then rearranged from positive and negative values to be only positive values (0 to 1 p.u.) because the block "PWM" and "PWM3" need only positive values. After that these signals are sent out to compare with the carrier for generating the output switching signals via SPWM ports. In addition, the output switching signals can be controlled to start or stop all PWM signals via SPWM ports by using control bit (logic "0" for start and logic "1" for stop) with the constant block "PWM Start".

After this software is compiled, dSPACE generates three extension file types, namely *.ppc file, *.sdf file and *.trc file. The *.ppc extension file is compiled to object file for execution on the dSPACE DS1104 controller board. The *.sdf extension file is a system description file. The *.trc extension file is a variable description file.

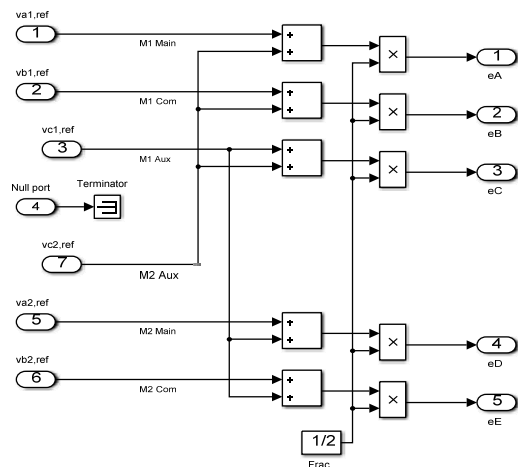


Fig. 15. Inside of the block "5-leg PWM Modulator".

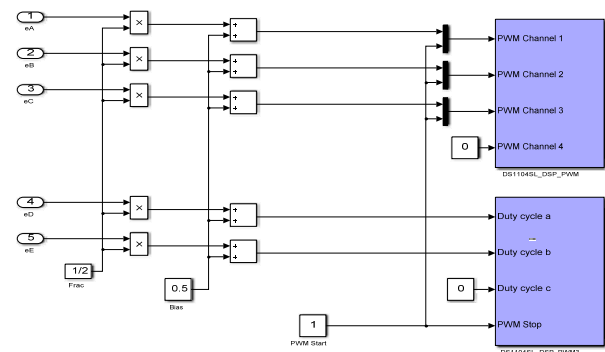


Fig. 16. Inside the block "5-leg PWM signal generator".

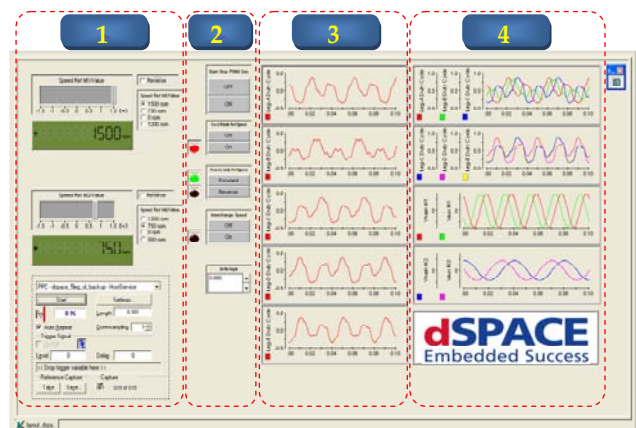


Fig. 17. Layout of dSPACE Control Desk for interfacing with the five-leg VSI.

Both *.sdf and *.trc extension files are necessary files for creating graphic user interface with control desk test automation software. The interfacing layout for controlling and monitoring variables of the proposed system is shown in Fig. 17.

The pattern of the interfacing layout of Fig. 17 has four parts. The first part (1) is speed commands for each motor (M1 and M2) which M1 speed command is at the upper part and the lower part is for M2 speed command. The second part (2) is control bit for test in case of study of Fig. 20 to 23 such as the command for simultaneously start or stop for both motor, the command for both speed reversal and so on. The third part (3) displays five voltage reference signals before rearranging the level of signals which the upper signal is phase reference voltage of leg A and the another signals are for leg B, C, D and E, respectively. The fourth part (4) shows the four groups of signals from top down to bottom which is rearranged level of voltage reference signals of leg A, B, C and Leg C, D, E, and the another signals are dq axis reference voltages for M1 and M2, respectively.

Experimental results and discussion

A. Steady state performance

The schematic diagram for the implementation of the proposed drive system using a five-leg VSI with a carrier-based SVPWM technique and corresponding photograph are shown in Fig. 18 (a) and Fig. 18 (b), respectively. Closed loop speed control, phase-leg reference signals and SVPWM signals are performed by only single dSPACE DS1104 DSP controller board with using a TMS320F240 slave DSP. Load 1 and 2 are induction generators coupled with both single-phase induction motors under test which parameters are illustrated in Table 1. The setting carrier frequency, f_c for the SVPWM is 1 kHz and the DC bus voltage is 310V.

In order to verify the correctness of the phase leg reference signals, the generated modulating signals are sent via a DAC port of the dSPACE for measurement by using a digital oscilloscope. Fig. 19 shows the measured results of the five modulating signals ($v_{A,ref}^*$, $v_{B,ref}^*$, $v_{C,ref}^*$, $v_{D,ref}^*$, $v_{E,ref}^*$) and

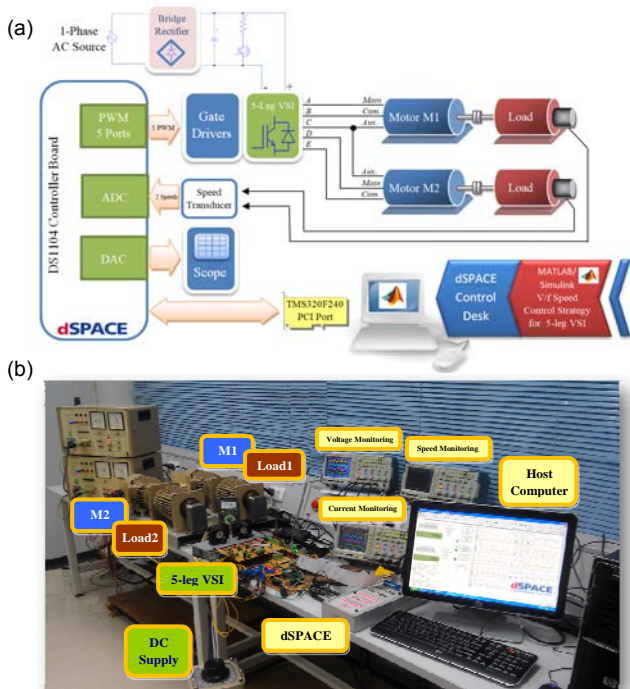


Fig. 18. Photograph of the hardware implementation of the proposed drive system. (a) Schematic diagram of the proposed system, (b) Hardware

corresponding reference voltages of main and auxiliary windings for the motor M1 and M2 with different magnitudes and frequencies at the same volts/Hz ($M_{a1}=1$, $f_1=50$ Hz, $M_{a2}=0.5$, $f_2=25$ Hz). The measured results are in good agreement. They confirm the correctness of the implementation.

Figs. 20 and 21 show waveforms and corresponding harmonic spectra of main and auxiliary winding voltages and currents for M1 and M2, respectively.

Clearly as shown in Fig.20(a) for M1 at 50 Hz and a certain load, the measured PWM voltage of the auxiliary winding leads that of the main winding by 90 degrees in accordance with Fig. 4(h) and (g) for the principle. Current waveforms of both windings are nearly sinusoidal with total harmonic distortion of 4.0616% and 9.9329%, for the main winding and auxiliary winding currents, respectively. The auxiliary winding current leads the main winding current about 90 degrees due to the lower ratio of X/R for the auxiliary winding. The amplitude of the auxiliary winding current is lower than that of the main winding current due to higher impedance as parameters illustrated in Table 1. Meanwhile, the waveforms of the motor M2 in Fig. 20 (b) are same behaviors as in Fig. 20(a) but the frequency is different with 25 Hz. However the auxiliary current waveform in Fig. 20 (b) is highly distorted with total harmonic distortion of 36.6% as shown in Fig.21(d).

B. Dynamic Response of Closed-loop speed control

For investigating the dynamic performance characteristics of the closed-loop speed control system shown in Fig. 18, the system has been tested with some conditions such as start-up, speed reversal, and so on.

Fig. 22 shows the speed response during start-up without load. For this test procedure, the reference speeds for M1 and M2 are set at 1,500 rpm and 750 rpm, respectively. The experimental results in Fig. 22 shows the responses of a step change in speed and corresponding winding current waveforms for both motors. The speed of M2 has slight overshoot. The speeds of both motors reach the reference values without steady state error. These confirm the effectiveness of the designed PI controllers. The starting currents about twice steady state values for both motors during start-up are obviously observed. Apparently, the response times of winding currents for M2 are faster than those for M1 since the reference speed of M2 is lower than that of M1. The proposed system is able to cope with the motor start-up.

Table 1. Single-phase induction motor parameters

Parameters	Resistance	Inductance
1ϕ , 370W, 230V, 1375rpm, 2.66A, 50Hz, 4 poles, $\alpha = 1.7723$		
Stator Main Winding	8.4 Ω	45.2275mH
Stator Auxiliary Winding	44.1 Ω	142.0539mH
Main Winding Rotor	16.8885 Ω	45.2275mH
Main Winding Mutual Inductance	-	507.7757mH

Fig. 23 shows the case of changing reference speed commands and also reversing speed direction, the proposed five-leg VSI drive system is able to independently control two single-phase induction motors according to the reference speed commands.

Fig. 23 (a) shows the multi-ranges of speed response of the shaft speeds for both motors. The motor M1 reference speed commands are set at 0 rpm, 1,500 rpm in the forward direction, 1,500 rpm in the reverse direction and finally 750 rpm in the reverse direction. The shaft speeds for both motors have been controlled to rotate according to the speed reference commands. However, both acceleration time and deceleration time for the shaft speed is about 2.5 seconds whilst both acceleration time and deceleration time for M2 are about 1 seconds. The currents of both windings for both motors in Fig. 23 (b) are increased during step

changes in speed and direction because of the required electromagnetic torque.

In case of the step change in load, Figs. 24 and 25 show the responses of the shaft speed and winding currents for both motors when either M1 or M2 is immediately loaded and released.

Clearly the winding currents particularly for M1 are increased and decreased during suddenly applied load and released load, respectively. The speeds are able to recover after disturbance.

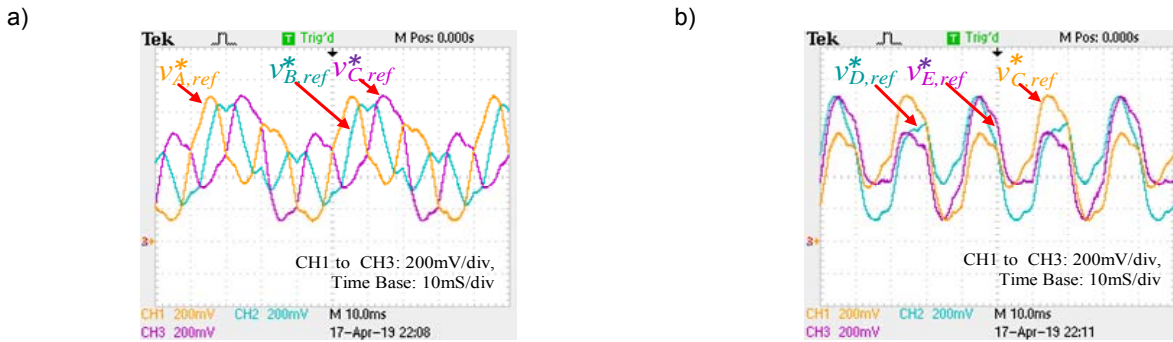


Fig. 19. Five phase leg reference voltage signals ($v_{A.ref}^*$, $v_{B.ref}^*$, $v_{C.ref}^*$, $v_{D.ref}^*$, $v_{E.ref}^*$) (a) $v_{A.ref}^*$, $v_{B.ref}^*$, $v_{C.ref}^*$, (b) $v_{C.ref}^*$, $v_{D.ref}^*$, $v_{E.ref}^*$.

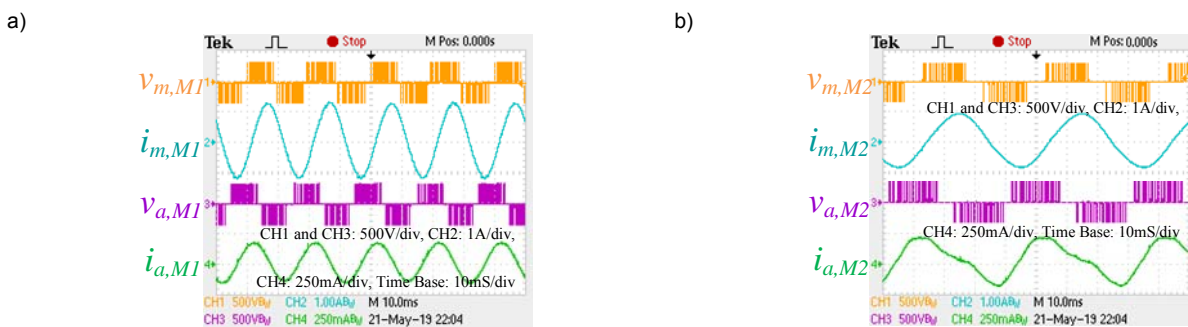


Fig. 20. Winding voltage and current waveforms of both motors on a certain load (a) Motor M1, (b) Motor M2.

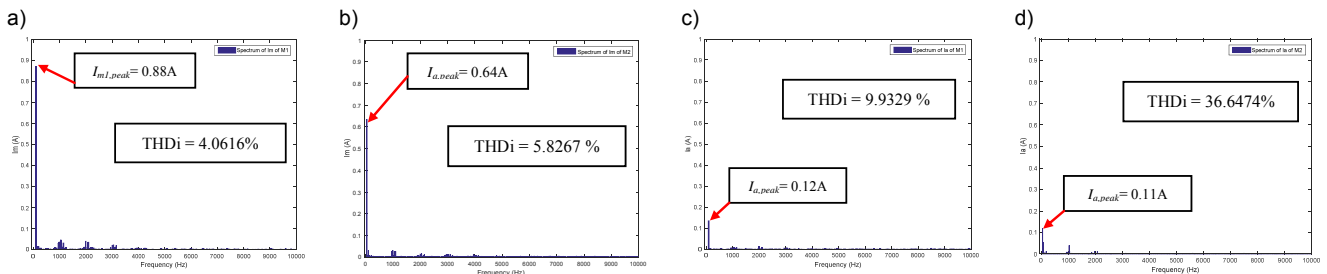


Fig. 21. Spectrums of Winding voltage and current waveforms of both motors during on load (a) M1 Main winding current spectrum, (b) M2 Main winding current spectrum, (c) M1 Aux winding current spectrum, (d) M2 Aux. winding current spectrum.

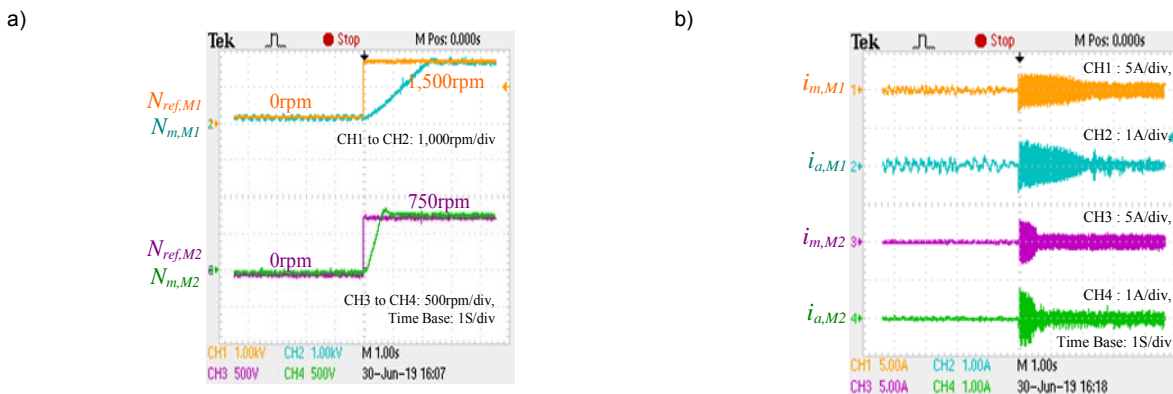


Fig. 22. Step speed change for each motor with different frequency and speed (a) reference and shaft speed, (b) winding currents.

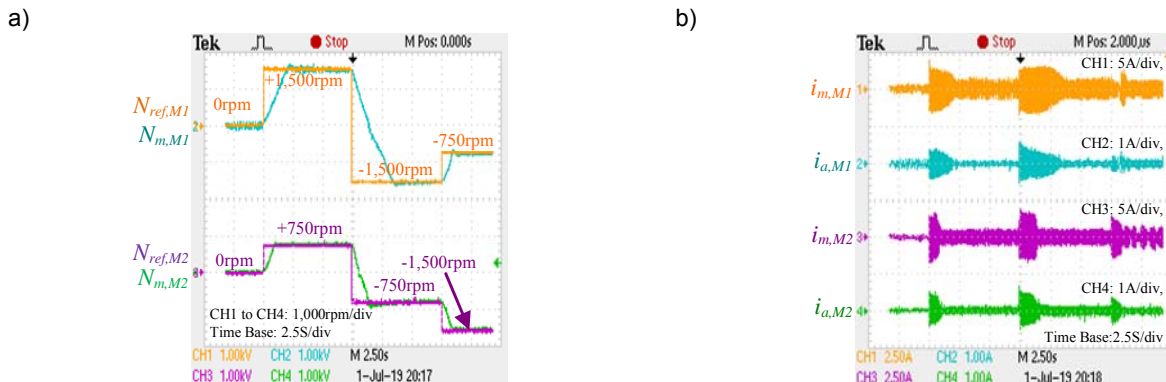


Fig. 23. Speed responses for each motor with different speeds and directions (a) reference and shaft speed, (b) winding currents.

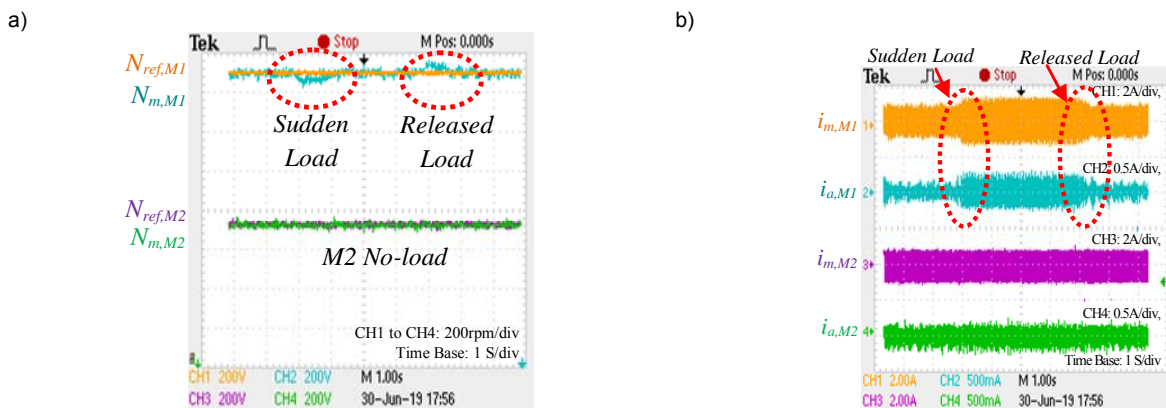


Fig. 24. Step load change on the motor M1 (a) reference and shaft speed, (b) winding

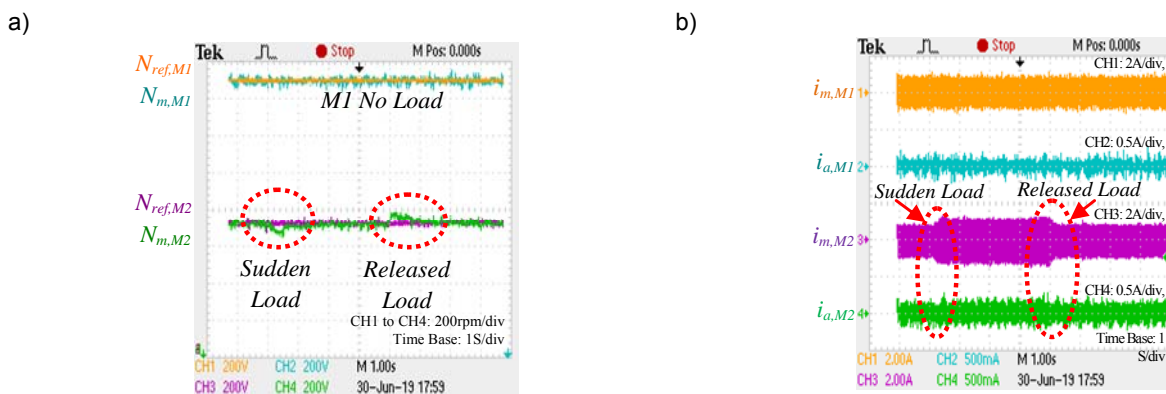


Fig. 25. Step load change on the motor M2 (a) reference and shaft speed, (b) winding currents.

Conclusions

This paper has proposed the implementation of a drive system of dual single-phase induction motor using a five-leg VSI with carrier-based SVPWM technique. A carrier based SVPWM technique for the proposed drive is employed. The advantages of the proposed drive system are independent closed loop speed control of both motors, a reduction in the number of switching devices thus reducing complexity, size, and cost. According to the experimental results, the implementation on hardware and software has shown that the capability of the proposed five-leg VSI drive system in terms of startup, step changes in load, speed command and direction is satisfactory.

Authors: Mr.Sirichai Dangeam, Department of Electrical Engineering, Faculty of Engineering, Rajamangala University of Technology Thanyaburi, E-mail: sirichai.d@en.rmutt.ac.th; Prof.Vijit Kinnares, Department of Electrical Engineering, Faculty of Engineering, King Mongkut's Institute of Technology Ladkrabang, E-mail: kkwijit@kmitl.ac.th.

REFERENCES

- [1] Lim, Y. S., Lee, J. S., Lee, K. B., Advanced speed control for a five-leg inverter driving a dual-induction motor system, *IEEE Trans. Ind. Electron.*, 66 (2019), No. 1, 707-716
- [2] Jones, M., Vukosavic, S. N., Dujic, D., Levi, E., Wright, P., Five-leg inverter PWM technique for reduced switch count two-motor constant power applications, *IET Electr. Power Appl.*, 2 (2008), No. 5, 275-287
- [3] Charumit, Ch., Kinnares, V., Carrier-based unbalanced phase voltage space vector PWM strategy for asymmetrical parameter type two-phase induction motor drives, *Science Direct, Electric Power Systems Research*, 79 (2009), No. 7, 1127-1135

- [4] Paweł, Ś., Marcin W., SVPWM algorithm in the scalar control structure for the three-phase voltage source inverter supplying two-phase high speed alternating current motors, *Przebieg Elektrotechniczny*, 86(2010), 311-317
- [5] Piyarat, W., Kinnares, V., Performance evaluation and slip regulation control of an asymmetrical parameter type two-phase induction motor drive using a three-leg voltage source inverter, *IEEJ Trans. Ind. Appl.*, 130 (2010), No. 7, 858-867
- [6] Kumsuwan, Y., Premrudeepreechacharn, S., Kinnares, V., A carrier-based unbalanced PWM method for four-leg voltage source inverter fed unsymmetrical two-phase induction motor, *IEEE Trans. Ind. Electron.*, 60 (2013), No. 5, 2031-2041
- [7] Mademlis, C., Kioskeridis, I., Theodoulidis, T., Optimization of single-phase induction motors-part I: maximum energy efficiency control, *IEEE Trans. Energy Convers.*, 20 (2005), No. 1, 187-195
- [8] Mademlis, C., Theodoulidis, T., Kioskeridis, I., Optimization of single-phase induction motors-part II: magnetic and torque performance under optimal control, *IEEE Trans. Energy Convers.*, 20 (2005), No. 1, 196-203
- [9] Abdel, R. N., Shaltout, A., An unsymmetrical two-phase induction motor drive with slip-frequency control, *IEEE Trans. Energy Convers.*, 24 (2009), No. 3, 608-616
- [10] Su, G. J., Hsu, J. S., A Five-leg inverter for driving a traction motor and a compressor motor, *IEEE Trans. Power Electron.*, 21 (2006), No. 3, 687-692
- [11] Talib, M.H.N., Ibrahim, Z., Rahim, N.A., Hasim, A.S.A., Characteristic of induction motor drives fed by three leg and five leg inverters, *Journal of Power Electronics*, 13 (2013), No. 5, 806-813
- [12] Talib, M.H.N., Ibrahim, Z., Rahim, N.A., Hasim, A.S.A., Implementation of space vector two-arm modulation for independent motor control drive fed by a five-leg inverter, *Journal of Power Electronics*, 14 (2014), No. 1, 115-124
- [13] Omata, R., Oka, K., Furuya, A., Matsumoto, S., Nozawa, Y., Matsuse, K., An improved performance of five-leg inverter in two induction motor drives, *CES/IEEE 5th International Power Electronics and Motion Control Conference*, 2006
- [14] Ledezma, E.; McGrath, B., Munoz, A., Lipo, T. A., Dual AC-drive system with a reduced switch count, *IEEE Trans. Ind. Appl.*, 37 (2001), No. 5, 1325-1333
- [15] Vukosavic, S. N., Jones, M., Dujic, D., Levi, E., An improved PWM method for a five-leg inverter supplying two three-phase motors, *ISIE 2008. IEEE International Symposium on Industrial Electronics*, 2008, 160-165
- [16] Tseng, S.K., Liu, T.H., Hsu, J.W., Ramelan, L. R., Firmansyah, E., Implementation of online maximum efficiency tracking control for a dual-motor drive system, *IET Electr. Power Appl.*, 9 (2015), No. 7, 449-458
- [17] Stanisław, P., Marcin W., SPWM and SVPWM methods for two- and three-leg VSI-fed two-phase high-speed AC motors and limitations associated with them, *Przebieg Elektrotechniczny*, 5a(2012), 208-217